Electronic Supplementary Material (ESI) for Physical Chemistry Chemical Physics.

SUPPLEMENTARY INFORMATION

Gas-phase reactivity of CH_3OH toward OH at interstellar temperatures (11.7-177.5 K): Experimental and theoretical study

Antonio J. Ocaña[1], Sergio Blázquez[1], Alexey Potapov[2], Bernabé Ballesteros[1,3], André Canosa[4], María Antiñolo[3], Luc Vereecken[5,*], José Albaladejo[1,3], Elena Jiménez[1,3,*]

1. *Departamento de Química Física. Facultad de Ciencias y Tecnologías Químicas. Universidad de Castilla-La Mancha, Avda. Camilo José Cela, 1B. 13071 Ciudad Real, Spain.*
1. *Laborastrophysikgruppe des Max-Planck-Instituts für Astronomie am Institut für Festkörperphysik, Friedrich-Schiller-Universität Jena, Helmholtzweg 3, 07743 Jena, Germany.*
2. *Instituto de Investigación en Combustión y Contaminación Atmosférica (ICCA). Universidad de Castilla-La Mancha, Avda. Moledores s/n. 13071 Ciudad Real, Spain.*
3. *Département de Physique Moléculaire, Institut de Physique de Rennes, UMR CNRS-UR1 6251, Université de Rennes 1, Campus de Beaulieu, 263 Avenue du Général Leclerc, 35042 Rennes Cedex, France.*
4. *Forschungszentrum Juelich GmbH, IEK-8. Wilhelm-Johnen-Straße 52425 Jülich, Germany.*

Aerodynamic characterization of new Laval nozzles (He-15K and Ar-100K)

The operational conditions of the He-15K and Ar-100 K nozzles are listed in Tables S1 and S2 and the spatial profile of T is depicted in Figs. S1 and S2 for all conditions used with both nozzles. For the rest of the investigated temperatures the previously characterized Laval nozzles He-23K-LP (low pressure), He-23K-IP (intermediate pressure), He-23K-HP (high pressure), He-36 K and Ar-50K were used.[1,2] When using the Ar-100K nozzle, the gas mixture was pulsed using the two-aperture rotatory disk (rotating at 5 Hz), as it was done for He-23K, He-36K and Ar-50K nozzles.[1] However, to achieve temperatures below 20 K (He-15K nozzle) with relatively low gas consumption and low pumping capacity, the disk with two apertures was replaced by a disk with one aperture of 16 mm×12 mm (length × height) dimensions which operates at 5 Hz.

Table S1 Summary of the operating conditions employed for the pulsed He-15K Laval nozzle.[a]

P_{res} / mbar	P_{cham}/ mbar	M	d_{max}/ cm	t_{hydro}/ μs	n / 10^{16} cm^{-3}	T/ K
366.48	0.117	8.58	53	307	6.88 ± 0.62	11.7 ± 0.7
280.16	0.117	8.04	38	223	6.41 ± 0.55	13.0 ± 0.7
236.75	0.122	7.75	32	186	5.90 ± 0.52	14.3 ± 0.8
140.81	0.071	7.05	41	443	1.91 ± 0.25	22.1 ± 1.4

^{a} Buffer gas is He (except for 22.1 K corresponding to a mixture of 50% N_2 and 50% He) and the temperature of the reservoir was constant (T_{res} = 297±2 K); Uncertainties in n and T are ±1σ (standard deviation) and represent the fluctuations of physical parameters along the length of uniformity of the flow.

Table S2 Summary of the operating conditions employed for the pulsed Ar-100K Laval nozzle. [a]

Buffer Gas	P_{res} /mbar	P_{cham}/mbar	M	d_{max}/ cm	t_{hydro}/ µs	n / 10^{16} cm^{-3}	T/ K
	109.73	5.960	2.65	18	387	43.38 ± 0.51	89.1 ± 0.7
	37.66	3.053	2.39	29	646	18.34 ± 0.17	101.8 ± 0.6
Ar	27.09	2.515	2.32	28	630	14.02 ± 0.11	106.0 ± 0.6
	16.16	1.964	2.16	27	625	9.58 ± 0.14	115.3 ± 1.1
	11.28	1.600	2.07	15	352	7.20 ± 0.08	122.5 ± 1.0
	71.99	5.200	2.43	16	277	24.92 ± 0.35	136.1 ± 0.8
	57.94	4.707	2.36	20	351	21.68 ± 0.40	140.4 ± 1.0
	43.77	3.822	2.32	22	389	17.02 ± 0.17	143.3 ± 0.6
N_2	29.10	2.923	2.24	27	485	12.35 ± 0.13	148.3 ± 0.6
	24.25	2.607	2.21	25	453	10.69 ± 0.12	149.9 ± 0.7
	19.42	2.281	2.15	23	424	9.14 ± 0.11	153.1 ± 0.7
	14.37	1.961	2.07	17	320	7.40 ± 0.07	158.8 ± 0.6
	9.96	1.566	1.98	10	192	5.64 ± 0.08	165.7 ± 0.9
	9.97	2.000	1.83	9	181	6.71 ± 0.11	177.5 ± 1.2

[a] The temperature of the reservoir was constant (T_{res} = 297±2 K); Uncertainties in n and T are ±1σ (standard deviation) and represent the fluctuations of physical parameters along the length of uniformity of the flow.

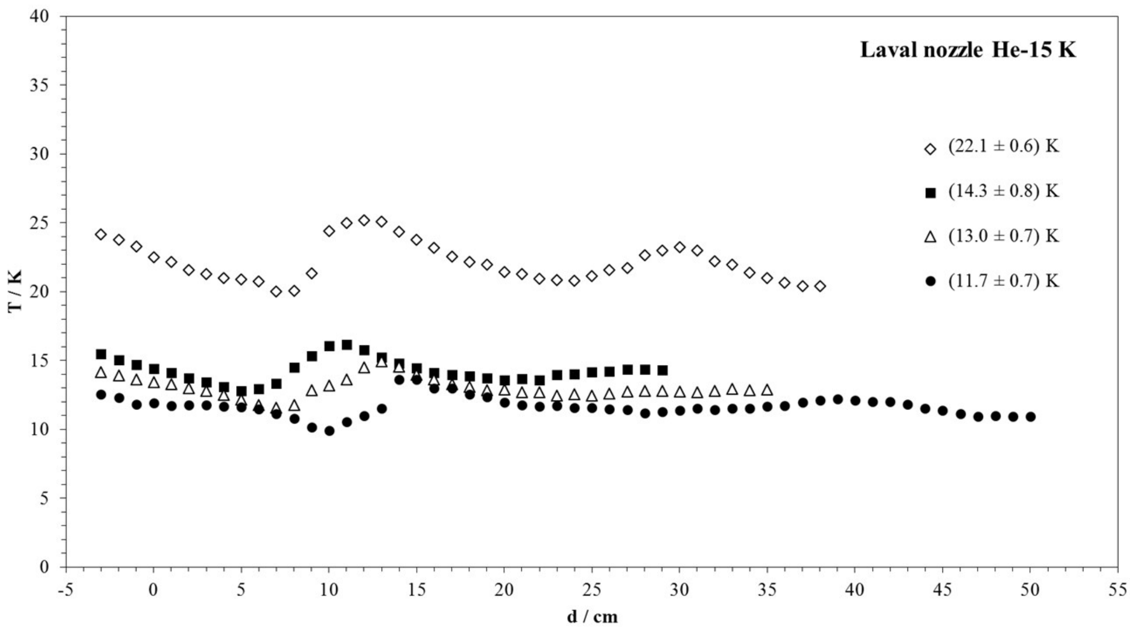

Fig. S1 Spatial profiles of the jet temperature obtained with the Laval nozzle He-15K.

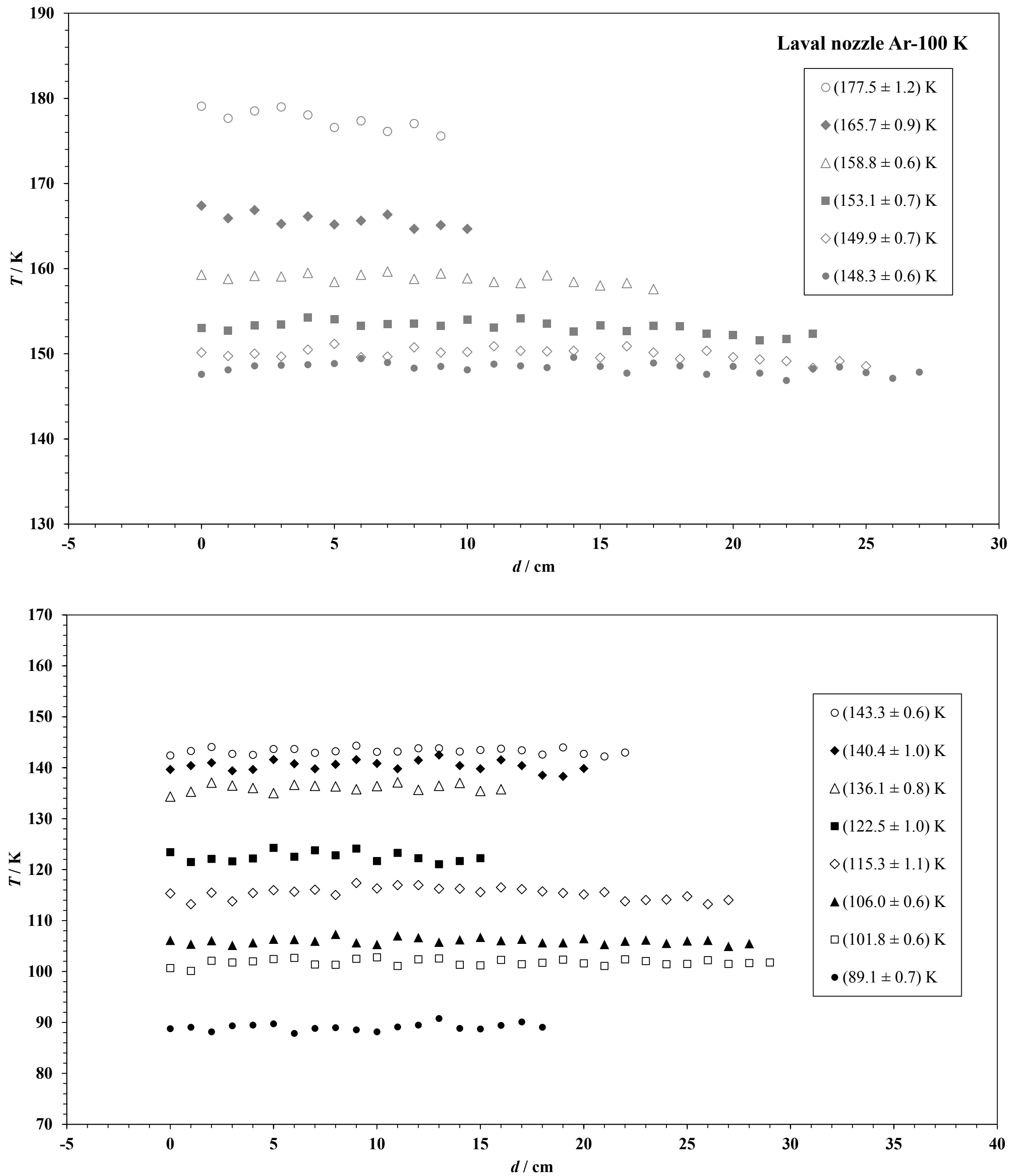

Fig. S2 Spatial profiles of the jet temperature obtained with the Laval nozzle Ar-100K.

Additionally to the Pitot measurements, the conventional pulsed laser photolysis-laser induced fluorescence (PLP-LIF) technique was used for recording the "ultra-cold" LIF spectrum of OH radicals between 281.0 and 282.8 nm with a spectral resolution of 0.002 nm or 0.004 nm at a fixed reaction time (40 μs). OH radicals were generated *in situ* in the jet by laser photolysis at 248 nm of a molecular precursor (H_2O_2 or tertbutyl hydroperoxide (t-BuOOH, $(CH_3)_3COOH$)). The LIF signal from OH radicals was monitored at ca. 309 nm, after laser excitation of electronic ground state OH at 282 nm. In Fig. S3, the recorded LIF spectrum at 11.7 K is shown together with the simulated one using LIFBASE software version 2.1 assuming thermalization of the system.[3]

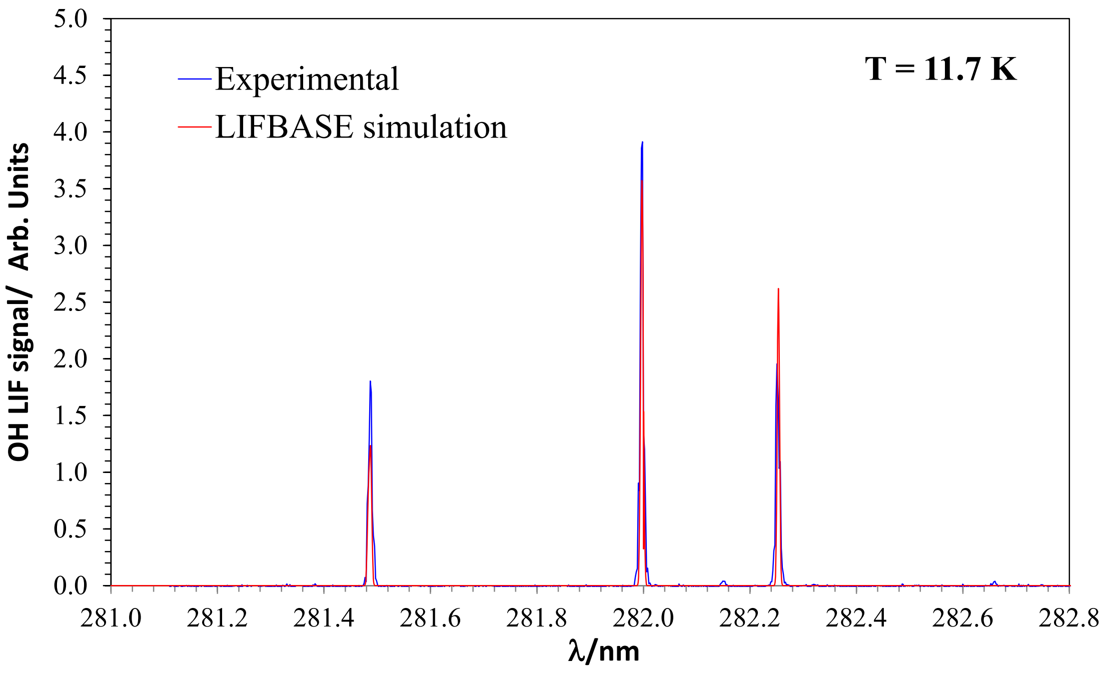

Fig. S3 Examples of the LIF spectrum of OH radicals recorded in the absence of methanol at 11.7 K and 40 μs delay time between the photolysis and the excitation lasers.

Determination of the methanol concentration by UV spectroscopy at 185 nm

Mixtures of gaseous methanol and a buffer gas (He, Ar or N_2) were prepared in a 50-L storage bulb. The dilution factor, *f*, in the bulb was calculated as $P_{methanol}/(P_{methanol}+P_{buffer})$ and ranged from 1.7×10^{-3} to 0.1. Typically, *f* was 1×10^{-2} (see Table S3). To check these values directly related to methanol concentration, UV spectroscopy at 185 nm was employed.

Introducing a known total pressure (P_{Total}) from the bulb in a 107-cm absorption cell, the absorbance ($A_{\lambda=185nm}$) was measured as $ln(I_0/I)$. The transmitted intensities at 185 nm from a Hg/Ar-pen ray in the absence and presence of methanol (I_0 and I, respectively) were detected in a filtered phototube. From the slope of the plots of the absorbance $A_{\lambda=185nm}$ versus P_{Total}, the dilution factor of methanol in the bulb was obtained:

$$A_{\lambda=185nm} = \frac{\sigma_{\lambda=185nm} \times l \times f}{RT} \times P_{Total} \tag{E.I}$$

using the absorption cross section (in base *e*), $\sigma_{\lambda=185nm} = 6.3\times10^{-19}$ cm^2 $molecule^{-1}$, reported at 185 nm by Jiménez et al.[4]. An example of the plots of eqn (E.I) is presented in Fig. S4. The good linearity implies that the Beer-Lambert law is valid in the concentration range in the absorption cell ($(1\text{-}6)\times10^{16}$ cm^{-3}).

References

1 E. Jiménez, B. Ballesteros, A. Canosa, T. M. Townsend, F. J. Maigler, V. Napal, B. R. Rowe and J. Albaladejo, Development of a pulsed uniform supersonic gas expansion system based on an aerodynamic chopper for gas phase reaction kinetic studies at ultra-low temperatures, *Rev. Sci. Instrum.*, 2015, **86**, 45108.

2 A. Canosa, A. J. Ocaña, M. Antiñolo, B. Ballesteros, E. Jiménez and J. Albaladejo, Design and testing of temperature tunable de Laval nozzles for applications in gas-phase reaction kinetics, *Exp. Fluids*, 2016, **57**, 1–14.

3 D. R. Luque, J. and Crosley, LIFBASE version 2.1 (SRI International, Menlo Park, CA, 1999), available at www.sri.com/psd/lifbase

4 E. Jiménez, M. K. Gilles and A. R. Ravishankara, Kinetics of the reactions of the hydroxyl radical with CH_3OH and C_2H_5OH between 235 and 360 K, *J. Photochem. Photobiol. A Chem.*, 2003, **157**, 237–245.

5 S. Xu and M. C. Lin, Theoretical study on the kinetics for OH reactions with CH_3OH and C_2H_5OH, *Proc. Combust. Inst.*, 2007, **31**, 159–166.

6 L. G. Gao, J. Zheng, A. Fernández-Ramos, D. G. Truhlar and X. Xu, Kinetics of the Methanol Reaction with OH at Interstellar, Atmospheric, and Combustion Temperatures, *J. Am. Chem. Soc.*, 2018, **140**, 2906–2918.

7 O. Roncero, A. Zanchet and A. Aguado, Low temperature reaction dynamics for CH_3OH + OH collisions on a new full dimensional potential energy surface, *Phys. Chem. Chem. Phys.*, 2018, **20**, 25951–25958.

8 W. Siebrand, Z. Smedarchina, E. Martínez-Núñez and A. Fernández-Ramos, Methanol dimer formation drastically enhances hydrogen abstraction from methanol by OH at low temperature, *Phys. Chem. Chem. Phys.*, 2016, **18**, 22712–22718.

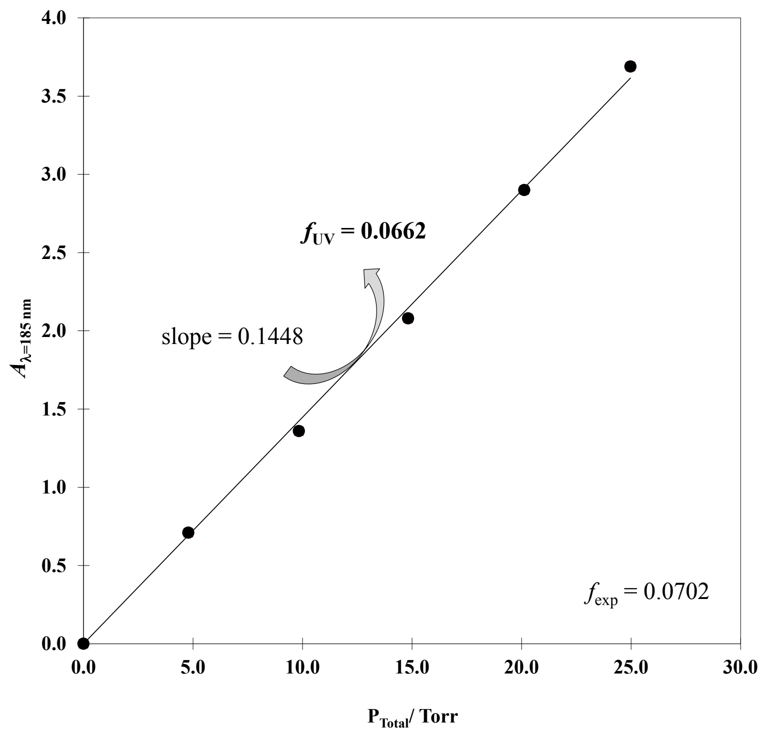

Fig. S4. Example of the measurement of the absorbance at 185 nm as a function of total pressure from a bulb with diluted methanol to check the dilution factor.

Table S3 Summary of the experimental conditions employed in the kinetic study: methanol dilution factor (*f*), mass flow rates (*F* in liters or cubic centimeters per minute – slpm or sccm- in standard conditions) and the range of methanol concentration used in the kinetic analysis.

T/ K	$f \times 10^{-3}$	F_{Buffer}/ slpm*	$F_{OH\text{-}precursor}$/ sccm	$F_{methanol/buffer}$/ sccm	$[CH_3OH]$/ 10^{14} cm^{-3}	% CH_3OH in the jet
11. 7 ± 0.7	5	5.05	100 [a]	80.8 – 423.3	0.05 – 0.28	0.008 – 0.041
13.0 ± 0.7	4 –14	3.84	100 [a]	80.3 – 718.1	0.06 – 0.40	0.010 – 0.060
14.3 ± 0.8	4	3.14	100 [a]	80.9 – 620.0	0.03 – 0.25	0.005 – 0.042
21.1 ± 0.6	6 – 54	5.80	20 [a]	50.3 – 715.9	0.09 – 0.63	0.035 – 0.188
21.7 ± 1.4	6 - 30	9.33	30 – 100 [a]	51.1 – 374.0	0.08 – 0.54	0.005 – 0.033
22.1 ± 1.4	8	2.58	50 [a]	80.6 – 373.1	0.09 – 0.41	0.047 – 0.213
22.5 ± 0.7	17 – 21	10.1	30 [a]	51.1 – 369.0	0.08 – 0.49	0.011 – 0.066
36.2 ± 1.2	5 – 8	12.6	70 [a]	101.4 – 557.7	0.06 – 0.51	0.003 – 0.029
45.3 ± 1.3	5 – 8	1.38	20 [a]	53.0 – 517.6	0.10 – 1.28	0.023 – 0.302
49.9 ± 1.4	5 – 10	3.91	20 [a]	71.1 – 694.6	0.08 – 1.45	0.009 – 0.174
50.5 ± 1.6	9 – 50	1.28	20 [a]	66.4 – 516.2	0.08 – 2.75	0.051 – 2.029
51.6 ± 1.7	13 – 73	12.8	50 – 200 [a]	64.7 – 1435.6	0.08 – 1.15	0.020 – 0.275
52.1 ± 0.5	5 – 15	4.63	20 – 30 [a]	30.3 – 121.1	0.09 – 0.44	0.005 – 0.023
64.1 ± 1.6	4 – 8	1.86	20 – 30 [a]	50.4 – 523.6	0.09 – 0.95	0.020 – 0.205
68.8 ± 0.6	13	5.04	20 [a]	31.0 – 123.6	0.14 – 0.54	0.008 – 0.033
69.5 ± 1.6	4 – 8	1.33	20 [a]	49.7 – 514.9	0.09 – 1.01	0.029 – 0.310
89.1 ± 0.7	6	7.79	50 [b]	49.9 – 220.2	0.15 – 0.66	0.003 – 0.015
89.5 ± 0.6	4	7.57	21 [a]	96.3 – 514.9	0.10 – 0.53	0.010 – 0.030

99.3 ± 0.4	4 – 8	2.46	12 [a]	49.7 – 467.4	0.07 – 1.17	0.010 – 0.150
101.8 ± 0.6	6	2.46	10 [a]	49.9 – 348.0	0.16 – 1.15	0.012 – 0.082
106.0 ± 0.6	5	1.73	5 [a]	50.7 – 557.8	0.21 – 2.29	0.015 – 0.163
107.0 ± 0.5	6 – 17	1.27	5 – 10 [a]	31.2 – 381.1	0.12 – 2.80	0.030 – 0.570
115.3 ± 1.1	8	0.96	2 [a]	49.8 – 432.1	0.39 – 3.07	0.041 – 0.321
122.5 ± 1.0	2– 15	0.63	4 [a, b]	49.4 – 302.0	0.84 – 5.11	0.117 – 0.709
136.1 ± 0.8	23	5.64	2 [a, b]	49.2 – 509.1	0.50 – 5.16	0.020 – 0.207
140.4 ± 1.0	55	4.43	10 [a, b]	48.3 – 499.3	1.32 – 13.6	0.061 – 0.625
143.3 ± 0.6	10	3.35	20 [a]	49.6 – 513.2	0.26 – 2.60	0.015 – 0.153
148.3 ± 0.6	30	2.19	4 [b]	48.6 – 378.8	0.83 – 6.41	0.067 – 0.519
149.9 ± 0.7	24	1.81	1 [a, b]	48.7 – 131.6	0.71 – 1.90	0.066 – 0.177
153.1 ± 0.7	30	1.42	2 [a, b]	48.6 – 420.1	0.94 – 8.04	0.103 – 0.880
158.8 ± 0.6	24	1.02	0.4 [a, b]	48.7 – 463.0	0.86 – 8.12	0.116 – 1.096
165.7 ± 0.9	50 – 100	0.67	0.4 – 1 [a, b]	46.8 – 251.9	2.00 – 11.1	0.354 – 1.972
177.5 ± 1.2	50 – 100	0.65	0.4 – 1 [a, b]	46.8 – 455.8	2.43 – 39.3	0.363 – 5.864

[*] In each kinetic experiment, the main flow ($\boldsymbol{F}_{\mathbf{Buffer}}$) was slightly changed when varying the methanol flow rate ($\boldsymbol{F}_{\mathbf{methanol/buffer}}$) in order to keep the $\boldsymbol{F}_{\mathbf{OH\text{-}precursor}}/\boldsymbol{F}_{\mathbf{Total}}$ ratio constant and, therefore, [OH-precursor] and k_0 constants; [a] H_2O_2; [b] *t*-BuOOH

Table S4 Predicted high-pressure rate coefficients (cm^3 molecule^{-1} s^{-1} for k_a and k_{HPL}; s^{-1} for k_{-a}, k_{b1} and k_{b2}) and product yields for the reaction steps in the CH_3OH + OH mechanism. k_{b1}(T) and k_{b2}(T) HPL predictions below 50K are considered unreliable (see main text) and are not reported.

T / K	k_a(T)	k_{-a}(T)	k_{b1}(T)	k_{b2}(T)	k_{HPL}(T)	Yield CH_2OH	Yield CH_3O
20	4.23×10^{-11}	1.92×10^{-40}			4.23×10^{-11}		
30	4.31×10^{-11}	1.02×10^{-22}			4.31×10^{-11}		
40	4.11×10^{-11}	8.22×10^{-14}			4.11×10^{-11}		
50	3.89×10^{-11}	1.90×10^{-8}	8.57×10^{-2}	5.74	3.89×10^{-11}	0.015	0.985
60	3.70×10^{-11}	7.31×10^{-5}	3.01×10^{-1}	16.5	3.70×10^{-11}	0.018	0.982
70	3.56×10^{-11}	2.69×10^{-2}	1.16	46.2	3.56×10^{-11}	0.025	0.975
80	3.45×10^{-11}	2.27	5.09	1.23×10^{2}	3.43×10^{-11}	0.040	0.960
90	3.37×10^{-11}	7.20×10	23.6	3.08×10^{2}	3.14×10^{-11}	0.071	0.929
100	3.32×10^{-11}	1.15×10^{3}	1.07×10^{2}	7.17×10^{2}	2.26×10^{-11}	0.130	0.870
110	3.28×10^{-11}	1.10×10^{4}	4.48×10^{2}	1.57×10^{3}	1.15×10^{-11}	0.222	0.778
120	3.25×10^{-11}	7.28×10^{4}	1.70×10^{3}	3.25×10^{3}	5.46×10^{-12}	0.343	0.657
130	3.23×10^{-11}	3.59×10^{5}	5.76×10^{3}	6.42×10^{3}	2.96×10^{-12}	0.473	0.527
140	3.22×10^{-11}	1.41×10^{6}	1.76×10^{4}	1.22×10^{4}	1.90×10^{-12}	0.591	0.409
150	3.22×10^{-11}	4.61×10^{6}	4.84×10^{4}	2.22×10^{4}	1.41×10^{-12}	0.685	0.315
160	3.22×10^{-11}	1.30×10^{7}	1.22×10^{5}	3.93×10^{4}	1.15×10^{-12}	0.756	0.244
170	3.23×10^{-11}	3.23×10^{7}	2.82×10^{5}	6.74×10^{4}	1.01×10^{-12}	0.807	0.193
180	3.23×10^{-11}	7.25×10^{7}	6.08×10^{5}	1.13×10^{5}	9.30×10^{-13}	0.844	0.156
190	3.25×10^{-11}	1.49×10^{8}	1.23×10^{6}	1.84×10^{5}	8.88×10^{-13}	0.870	0.130
200	3.26×10^{-11}	2.85×10^{8}	2.34×10^{6}	2.92×10^{5}	8.70×10^{-13}	0.889	0.111
210	3.28×10^{-11}	5.12×10^{8}	4.23×10^{6}	4.55×10^{5}	8.68×10^{-13}	0.903	0.097
220	3.29×10^{-11}	8.69×10^{8}	7.31×10^{6}	6.93×10^{5}	8.77×10^{-13}	0.913	0.087
230	3.31×10^{-11}	1.41×10^{9}	1.21×10^{7}	1.03×10^{6}	8.95×10^{-13}	0.921	0.079
240	3.33×10^{-11}	2.18×10^{9}	1.94×10^{7}	1.52×10^{6}	9.21×10^{-13}	0.928	0.072
250	3.34×10^{-11}	3.27×10^{9}	3.01×10^{7}	2.18×10^{6}	9.52×10^{-13}	0.932	0.068
260	3.36×10^{-11}	4.73×10^{9}	4.53×10^{7}	3.08×10^{6}	9.89×10^{-13}	0.936	0.064

270	3.38×10^{-11}	6.65×10^{9}	6.63×10^{7}	4.28×10^{6}	1.03×10^{-12}	0.939	0.061
280	3.40×10^{-11}	9.11×10^{9}	9.48×10^{7}	5.86×10^{6}	1.08×10^{-12}	0.942	0.058
290	3.42×10^{-11}	1.22×10^{10}	1.32×10^{8}	7.91×10^{6}	1.12×10^{-12}	0.944	0.056
300	3.43×10^{-11}	1.60×10^{10}	1.82×10^{8}	1.05×10^{7}	1.18×10^{-12}	0.945	0.055
310	3.45×10^{-11}	2.05×10^{10}	2.44×10^{8}	1.38×10^{7}	1.23×10^{-12}	0.947	0.053
320	3.46×10^{-11}	2.59×10^{10}	3.23×10^{8}	1.79×10^{7}	1.29×10^{-12}	0.947	0.053
330	3.48×10^{-11}	3.22×10^{10}	4.21×10^{8}	2.30×10^{7}	1.36×10^{-12}	0.948	0.052
340	3.49×10^{-11}	3.95×10^{10}	5.41×10^{8}	2.91×10^{7}	1.42×10^{-12}	0.949	0.051
350	3.51×10^{-11}	4.78×10^{10}	6.87×10^{8}	3.66×10^{7}	1.49×10^{-12}	0.949	0.051
360	3.52×10^{-11}	5.71×10^{10}	8.60×10^{8}	4.55×10^{7}	1.57×10^{-12}	0.950	0.050
370	3.53×10^{-11}	6.75×10^{10}	1.07×10^{9}	5.60×10^{7}	1.64×10^{-12}	0.950	0.050
380	3.54×10^{-11}	7.90×10^{10}	1.31×10^{9}	6.84×10^{7}	1.72×10^{-12}	0.950	0.050
390	3.55×10^{-11}	9.15×10^{10}	1.59×10^{9}	8.28×10^{7}	1.80×10^{-12}	0.950	0.050

Table S5 Predicted low-pressure limit rate coefficient (k_{LPL}(T) in cm^3 $molecule^{-1}$ s^{-1}) and product yields for the reaction steps in the CH_3OH + OH mechanism.

T / K	k_{LPL}(T)	CH_2OH Yield	CH_3O Yield
20	2.29×10^{-11}	0.711	0.289
30	1.47×10^{-11}	0.712	0.288
40	9.35×10^{-12}	0.713	0.287
50	6.19×10^{-12}	0.714	0.286
60	4.30×10^{-12}	0.715	0.285
70	3.13×10^{-12}	0.716	0.284
80	2.37×10^{-12}	0.717	0.283
90	1.86×10^{-12}	0.718	0.282
100	1.50×10^{-12}	0.719	0.281
110	1.25×10^{-12}	0.721	0.279
120	1.06×10^{-12}	0.723	0.277
130	9.15×10^{-13}	0.725	0.275
140	8.08×10^{-13}	0.727	0.273
150	7.26×10^{-13}	0.730	0.270
160	6.63×10^{-13}	0.733	0.267
170	6.14×10^{-13}	0.736	0.264
180	5.77×10^{-13}	0.740	0.260
190	5.48×10^{-13}	0.744	0.256
200	5.27×10^{-13}	0.748	0.252
210	5.13×10^{-13}	0.752	0.248
220	5.03×10^{-13}	0.757	0.243
230	4.98×10^{-13}	0.762	0.238
240	4.96×10^{-13}	0.767	0.233
250	4.98×10^{-13}	0.772	0.228
260	5.03×10^{-13}	0.776	0.224
270	5.11×10^{-13}	0.781	0.219
280	5.21×10^{-13}	0.786	0.214
290	5.34×10^{-13}	0.791	0.209
300	5.49×10^{-13}	0.795	0.205
310	5.66×10^{-13}	0.800	0.200
320	5.85×10^{-13}	0.804	0.196
330	6.06×10^{-13}	0.808	0.192
340	6.29×10^{-13}	0.812	0.188
350	6.53×10^{-13}	0.815	0.185
360	6.79×10^{-13}	0.819	0.181
370	7.07×10^{-13}	0.822	0.178
380	7.37×10^{-13}	0.825	0.175
390	7.68×10^{-13}	0.828	0.172

Table S6 Predicted high- and low-pressure rate coefficients (cm^3 molecule^{-1} s^{-1} for k_a and k_{HPL}; s^{-1} for k_{-a}, k_{b1} and k_{b2}) and product yields for the reaction steps in the CH_3OH + OH mechanism, after adjustment of the barrier heights for H-abstraction to match the IUPAC k(300K) and the CH_3O yield recommendations, and scaling the low-energy capture rate coefficient to the average of the experimental k(20K) values. CH_2OH and CH_3O HPL yields below 50K are considered unreliable (see main text) and are not reported.

T / K	$k_{capture}$(T)	k_{HPL}(T)	CH_2OH Yield HPL	CH_3O Yield HPL	k_{LPL}(T)	CH_2OH Yield LPL	CH_3O Yield LPL
20	**6.79×10^{-11}**	6.79×10^{-11}			3.39×10^{-11}	0.503	0.497
30	6.46×10^{-11}	6.46×10^{-11}			2.18×10^{-11}	0.505	0.495
40	5.68×10^{-11}	5.68×10^{-11}			1.35×10^{-11}	0.508	0.492
50	4.96×10^{-11}	4.96×10^{-11}	0.000	1.000	8.55×10^{-12}	0.511	0.489
60	4.42×10^{-11}	4.42×10^{-11}	0.000	1.000	5.64×10^{-12}	0.513	0.487
70	4.04×10^{-11}	4.04×10^{-11}	0.000	1.000	3.93×10^{-12}	0.516	0.484
80	3.78×10^{-11}	3.78×10^{-11}	0.001	0.999	2.87×10^{-12}	0.519	0.481
90	3.60×10^{-11}	3.58×10^{-11}	0.002	0.998	2.18×10^{-12}	0.523	0.477
100	3.48×10^{-11}	3.29×10^{-11}	0.005	0.995	1.72×10^{-12}	0.526	0.474
110	3.39×10^{-11}	2.60×10^{-11}	0.014	0.986	1.40×10^{-12}	0.531	0.469
120	3.34×10^{-11}	1.57×10^{-11}	0.031	0.969	1.17×10^{-12}	0.535	0.465
130	3.30×10^{-11}	8.03×10^{-12}	0.065	0.935	1.00×10^{-12}	0.540	0.460
140	3.27×10^{-11}	4.17×10^{-12}	0.118	0.882	8.75×10^{-13}	0.546	0.454
150	3.26×10^{-11}	2.42×10^{-12}	0.191	0.809	7.78×10^{-13}	0.552	0.448
160	3.25×10^{-11}	1.59×10^{-12}	0.279	0.721	7.04×10^{-13}	0.559	0.441
170	3.25×10^{-11}	1.18×10^{-12}	0.371	0.629	6.46×10^{-13}	0.566	0.434
180	3.25×10^{-11}	9.53×10^{-13}	0.459	0.541	6.02×10^{-13}	0.574	0.426
190	3.26×10^{-11}	8.30×10^{-13}	0.536	0.464	5.68×10^{-13}	0.582	0.418
200	3.27×10^{-11}	7.62×10^{-13}	0.602	0.398	5.43×10^{-13}	0.592	0.408
210	3.29×10^{-11}	7.28×10^{-13}	0.656	0.344	5.24×10^{-13}	0.601	0.399
220	3.30×10^{-11}	7.14×10^{-13}	0.699	0.301	5.11×10^{-13}	0.611	0.389
230	3.32×10^{-11}	7.16×10^{-13}	0.734	0.266	5.02×10^{-13}	0.621	0.379
240	3.33×10^{-11}	7.28×10^{-13}	0.762	0.238	4.98×10^{-13}	0.632	0.368
250	3.35×10^{-11}	7.48×10^{-13}	0.785	0.215	4.97×10^{-13}	0.642	0.358
260	3.37×10^{-11}	7.74×10^{-13}	0.803	0.197	5.00×10^{-13}	0.652	0.348

270	3.38×10^{-11}	8.06×10^{-13}	0.818	0.182	5.06×10^{-13}	0.663	0.337
280	3.40×10^{-11}	8.43×10^{-13}	0.831	0.169	5.14×10^{-13}	0.673	0.327
290	3.42×10^{-11}	8.84×10^{-13}	0.842	0.158	5.25×10^{-13}	0.683	0.317
300	3.43×10^{-11}	$\mathbf{9.28\times10^{-13}}$	0.850	**0.150**	5.38×10^{-13}	0.692	0.308
310	3.45×10^{-11}	9.77×10^{-13}	0.858	0.142	5.53×10^{-13}	0.702	0.298
320	3.47×10^{-11}	1.03×10^{-12}	0.864	0.136	5.70×10^{-13}	0.711	0.289
330	3.48×10^{-11}	1.08×10^{-12}	0.870	0.130	5.89×10^{-13}	0.719	0.281
340	3.49×10^{-11}	1.14×10^{-12}	0.875	0.125	6.10×10^{-13}	0.728	0.272
350	3.51×10^{-11}	1.20×10^{-12}	0.879	0.121	6.33×10^{-13}	0.735	0.265
360	3.52×10^{-11}	1.27×10^{-12}	0.882	0.118	6.58×10^{-13}	0.743	0.257
370	3.53×10^{-11}	1.34×10^{-12}	0.886	0.114	6.84×10^{-13}	0.750	0.250
380	3.54×10^{-11}	1.41×10^{-12}	0.888	0.112	7.12×10^{-13}	0.757	0.243
390	3.56×10^{-11}	1.48×10^{-12}	0.891	0.109	7.42×10^{-13}	0.763	0.237

Values in bold are the fitted values.

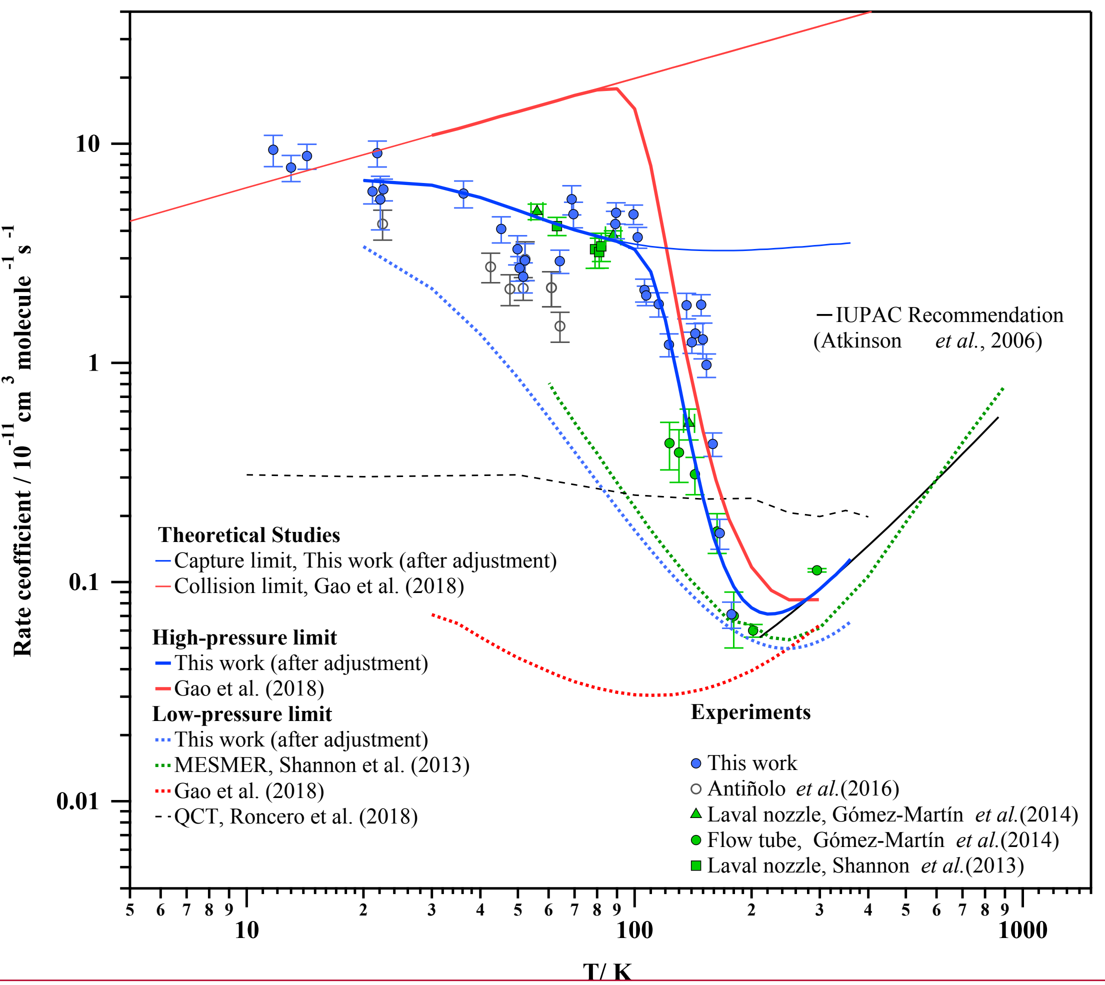
Rate ceofficient / 10^-11 cm^3 molecule^-1 s^-1
T/ K
IUPAC Recommendation (Atkinson et al., 2006)
Theoretical Studies
Capture limit, This work (after adjustment)
Collision limit, Gao et al. (2018)
High-pressure limit
This work (after adjustment)
Gao et al. (2018)
Low-pressure limit
This work (after adjustment)
MESMER, Shannon et al. (2013)
Gao et al. (2018)
QCT, Roncero et al. (2018)
Experiments
This work
Antiñolo et al.(2016)
Laval nozzle, Gómez-Martín et al.(2014)
Flow tube, Gómez-Martín et al.(2014)
Laval nozzle, Shannon et al.(2013)

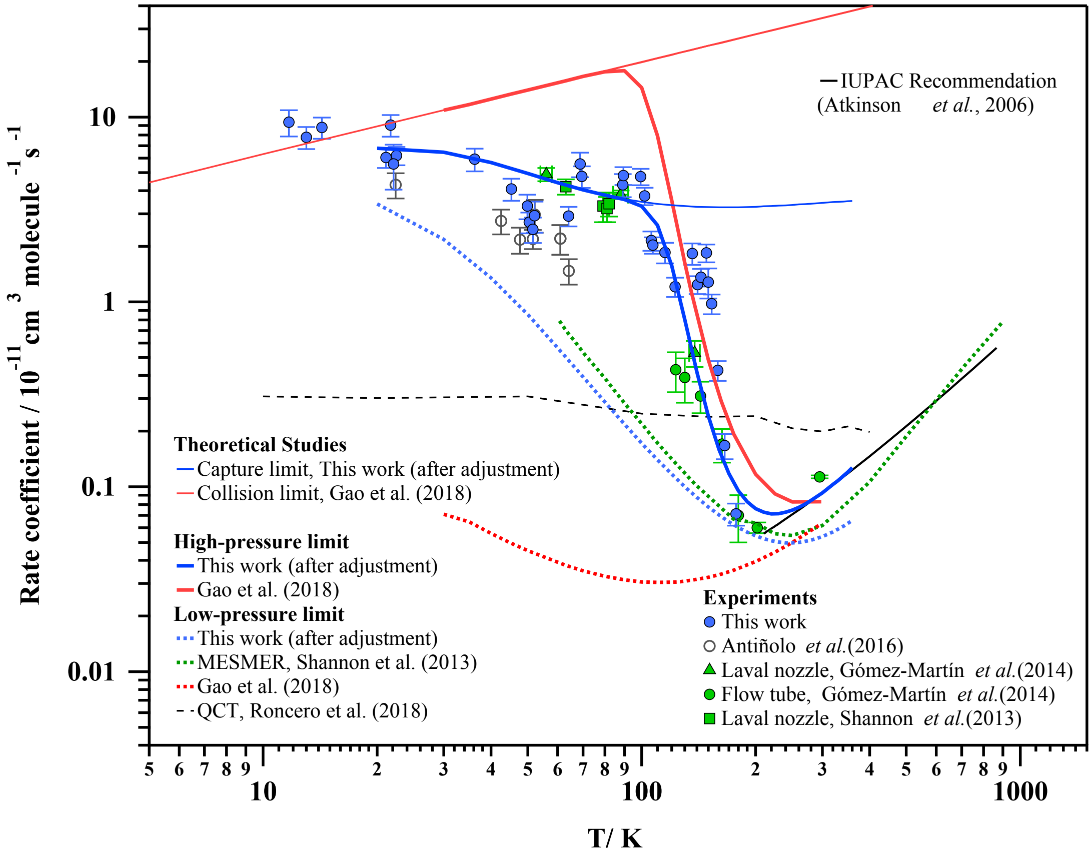

Fig. S5 Theoretically predicted capture-, high-pressure, and low-pressure rate coefficients (cm^3 molecule^{-1} s^{-1}) for the CH_3OH + OH reactions, after adjustment of the barrier heights for H-abstraction to match the IUPAC k(300K) and Y(CH_3O+H_2O) recommendations, and scaling the low-energy k(E) capture rate coefficient to the average of the experimental k(20K) values.

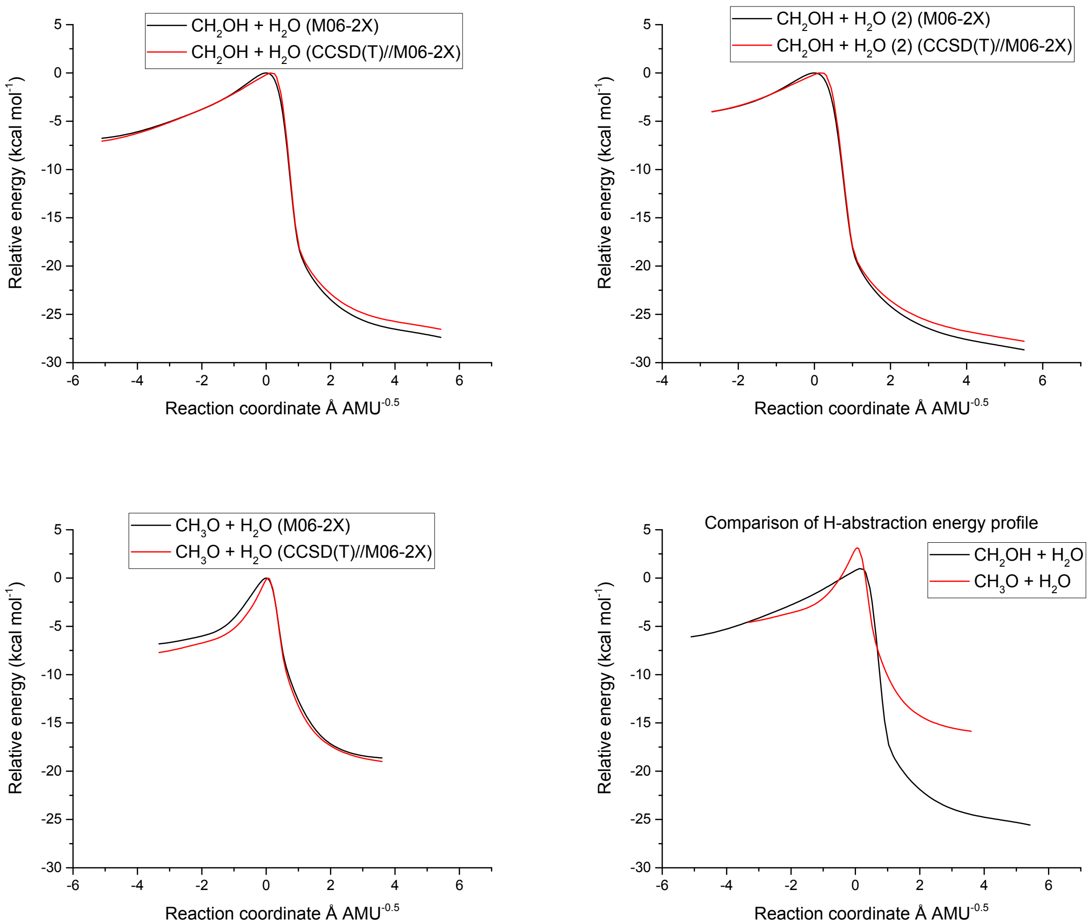

Fig. S6 IRC energy profiles at the M06-2X/aug-cc-pVTZ and CCSD(T)//aug-cc-pVTZ//M06-2X levels of theory. Top left and right: 2 TS conformers for methyl-H abstraction. Bottom left: Lowest-energy TS conformer for hydroxy-H-abstraction. Bottom right: side-by-side comparison of the CCSD(T)//M06-2X energy profiles for the lowest-energy conformers of the two classes of H-abstraction.

Table S7 Relative energies (kcal mol^{-1}) for the critical points on the potential energy surface for the CH_3OH + OH reaction, at various selected levels of theory as available in this work and the literature. The values in bold are used in the kinetic analysis in this work.

Methodology	Reactants	Complex	TS_{b1}	TS_{b2}	Reference
M06-2X/aug-cc-pVQZ	0.00	-4.96	0.23	0.92	This work
CCSD(T)/aug-cc-pVQZ//M06-2X/aug-cc-pVQZ	0.00	-4.87	1.04	2.91	This work
IRCMax(CCSD(T)/aug-cc-pVTZ //M06-2X/ aug-cc-pVQZ)	0.00	-5.00	1.11	2.71	This work
CCSD(T)/CBS(DTQ)// IRCMax(CCSD(T)/aug-cc-pVTZ// M06-2X/ aug-cc-pVQZ)	**0.00**	**-4.75**	**0.98**	**3.13**	This work
B3LYP-D3/aug-cc-pVQZ	0.00		-2.55	-5.19	This work
IRCMax(CCSD(T)/aug-cc-pVTZ//B3LYP-D3/aug-cc-pVQZ)	0.00		2.77	3.38	This work
ωB97XD/aug-cc-pVQZ	0.00		-1.27	-1.01	This work
IRCMax(CCSD(T)/aug-cc-pVTZ//ωB97XD/aug-cc-pVQZ)	0.00		1.99	2.81	This work
CCSD(T)/6-311+G(3df,2p)//MP2/6-311+G(3df,2p)	0.00	-4.9	1.0	3.6	Xu and Lin[5]
CCSD(T)-F12a/jun-cc-pVTZ//M08-HX/MG3S	0.00		1.46	3.06	Gao et al.[6]
CCSD(T)/jun-cc-pVTZ//M08-HX/MG3S	0.00	-6.48			Gao et al.[6]
CASPT2(11,11)/MG3S//M08-HX/MG3S	0.00			3.06	Gao et al.[6]
CCSD(T)-F12a/cc-pVDZ-F12	0.00	-6.46	2.14	6.22	Roncero et al.[7]
MRCI-F12+Q/cc-pVDZ-F12	0.00	-6.39	1.52	5.30	Roncero et al.[7]
MPWB1K/6-31+G(d,p)	0.00	-5.64	0.14	1.17	Siebrand et al.[8]

Raw quantum chemical information

```
**********************************************
CH3OH + OH : M06-2X/aug-cc-pVQZ geometry
**********************************************

CH3OH
-------------------------------
E(CCSD(T)/Aug-CC-pVDZ) (Hartree): -115.45498354
E(CCSD/Aug-CC-pVDZ) (Hartree): -115.44462500
     T1 diagnostic:  0.010890
E(MP2/Aug-CC-pVDZ) (Hartree): -115.42130425
E(MP3/Aug-CC-pVDZ) (Hartree): -115.43932083
E(RHF/Aug-CC-pVDZ) (Hartree): -115.06185312
E(CCSD(T)/Aug-CC-pVTZ) (Hartree): -115.56223795
E(CCSD/Aug-CC-pVTZ) (Hartree): -115.54646879
     T1 diagnostic:  0.009855
E(MP2/Aug-CC-pVTZ) (Hartree): -115.52891141
E(MP3/Aug-CC-pVTZ) (Hartree): -115.54321870
E(RHF/Aug-CC-pVTZ) (Hartree): -115.09250401
E(CCSD(T)/Aug-CC-pVQZ) (Hartree): -115.59312236
E(CCSD/Aug-CC-pVQZ) (Hartree): -115.57611768
     T1 diagnostic:  0.009595
E(MP2/Aug-CC-pVQZ) (Hartree): -115.56306030
E(MP3/Aug-CC-pVQZ) (Hartree): -115.57360507
E(RHF/Aug-CC-pVQZ) (Hartree): -115.10002664
E(RM062X/Aug-CC-pVQZ) (Hartree): -115.72433910
Point group : CS
Electronic state : 1-A'
Cartesian coordinates (Angs):
     C       0.046385      0.660592      -0.000000
     O       0.046385     -0.751993       0.000000
     H      -0.438149      1.069902       0.888635
     H       1.085396      0.977752       0.000000
     H      -0.438149      1.069902      -0.888635
     H      -0.858491     -1.065162       0.000000
Rotational constants (GHz):  129.3682900   25.0088300   24.1448400
Vibrational harmonic frequencies (cm-1):
      294.3065 (  A")          1070.1678 (  A')          1113.3611 (  A')
     1184.7692 (  A")          1370.3871 (  A')          1488.4511 (  A')
     1511.0638 (  A")          1520.8251 (  A')          3039.2214 (  A')
     3091.6887 (  A")          3150.9860 (  A')          3907.2995 (  A')
Zero-point correction (Hartree): 0.051811

OH
-------------------------------
E(CCSD(T)/Aug-CC-pVDZ) (Hartree):  -75.58401208
E(CCSD/Aug-CC-pVDZ) (Hartree):  -75.58065075
     T1 diagnostic:  0.012115
E(MP2/Aug-CC-pVDZ) (Hartree):  -75.56555498
E(MP3/Aug-CC-pVDZ) (Hartree):  -75.57785261
E(PMP2/Aug-CC-pVDZ) (Hartree):  -75.56731410
E(PMP3/Aug-CC-pVDZ) (Hartree):  -75.57891269
E(PUHF/Aug-CC-pVDZ) (Hartree):  -75.40654471
E(UHF/Aug-CC-pVDZ) (Hartree):  -75.40362085
E(CCSD(T)/Aug-CC-pVTZ) (Hartree):  -75.64558106
E(CCSD/Aug-CC-pVTZ) (Hartree):  -75.63969742
     T1 diagnostic:  0.010018
E(MP2/Aug-CC-pVTZ) (Hartree):  -75.62633534
E(MP3/Aug-CC-pVTZ) (Hartree):  -75.63790257
E(PMP2/Aug-CC-pVTZ) (Hartree):  -75.62832327
E(PMP3/Aug-CC-pVTZ) (Hartree):  -75.63904324
E(PUHF/Aug-CC-pVTZ) (Hartree):  -75.42495141
```

```
E(UHF/Aug-CC-pVTZ) (Hartree):  -75.42160059
E(CCSD(T)/Aug-CC-pVQZ) (Hartree):  -75.66449481
E(CCSD/Aug-CC-pVQZ) (Hartree):  -75.65801686
     T1 diagnostic:  0.009499
E(MP2/Aug-CC-pVQZ) (Hartree):  -75.64662073
E(MP3/Aug-CC-pVQZ) (Hartree):  -75.65673028
E(PMP2/Aug-CC-pVQZ) (Hartree):  -75.64863276
E(PMP3/Aug-CC-pVQZ) (Hartree):  -75.65786986
E(PUHF/Aug-CC-pVQZ) (Hartree):  -75.42997948
E(UHF/Aug-CC-pVQZ) (Hartree):  -75.42659099
E(UM062X/Aug-CC-pVQZ) (Hartree):  -75.73716255
Point group : C*V
Cartesian coordinates (Angs):
     O       0.000000      0.000000       0.107876
     H       0.000000      0.000000      -0.863009
Rotational constants (GHz):    0.0000000  565.5013271  565.5013271
Vibrational harmonic frequencies (cm-1):
     3774.9088 (  SG)
Zero-point correction (Hartree): 0.008600

complex.CH3OH.OH
-------------------------------
E(CCSD(T)/Aug-CC-pVDZ) (Hartree): -191.04949837
E(CCSD/Aug-CC-pVDZ) (Hartree): -191.03525841
     T1 diagnostic:  0.011561
E(MP2/Aug-CC-pVDZ) (Hartree): -190.99741315
E(MP3/Aug-CC-pVDZ) (Hartree): -191.02737930
E(PMP2/Aug-CC-pVDZ) (Hartree): -190.99913117
E(PMP3/Aug-CC-pVDZ) (Hartree): -191.02840916
E(PUHF/Aug-CC-pVDZ) (Hartree): -190.47587267
E(UHF/Aug-CC-pVDZ) (Hartree): -190.47298309
E(CCSD(T)/Aug-CC-pVTZ) (Hartree): -191.21842864
E(CCSD/Aug-CC-pVTZ) (Hartree): -191.19626132
     T1 diagnostic:  0.010175
E(MP2/Aug-CC-pVTZ) (Hartree): -191.16590803
E(MP3/Aug-CC-pVTZ) (Hartree): -191.19151288
E(PMP2/Aug-CC-pVTZ) (Hartree): -191.16785052
E(PMP3/Aug-CC-pVTZ) (Hartree): -191.19262190
E(PUHF/Aug-CC-pVTZ) (Hartree): -190.52465603
E(UHF/Aug-CC-pVTZ) (Hartree): -190.52134495
E(CCSD(T)/Aug-CC-pVQZ) (Hartree): -191.26802431
E(CCSD/Aug-CC-pVQZ) (Hartree): -191.24402370
     T1 diagnostic:  0.009785
E(MP2/Aug-CC-pVQZ) (Hartree): -191.22019895
E(MP3/Aug-CC-pVQZ) (Hartree): -191.24055607
E(PMP2/Aug-CC-pVQZ) (Hartree): -191.22216429
E(PMP3/Aug-CC-pVQZ) (Hartree): -191.24166384
E(PUHF/Aug-CC-pVQZ) (Hartree): -190.53713445
E(UHF/Aug-CC-pVQZ) (Hartree): -190.53378740
E(UM062X/Aug-CC-pVQZ) (Hartree): -191.47204925
Electronic state : 2-A
Cartesian coordinates (Angs):
     C      -1.376251     -0.497243       0.004285
     O      -0.542169      0.650622      -0.023596
     H      -2.098571     -0.483942      -0.811689
     H      -0.725213     -1.358128      -0.116930
     H      -1.902267     -0.586095       0.954668
     H      -1.064318      1.443143       0.104014
     H       1.261635      0.246727      -0.001102
     O       2.140449     -0.185402       0.004262
Rotational constants (GHz):   30.7119500    4.4599000    3.9937600
Vibrational harmonic frequencies (cm-1):
       43.6350                  52.9643                  211.9748
```

```
     290.6564                  386.3313                  607.9129
    1079.4094                 1099.4822                 1187.0870
    1367.0626                 1490.5108                 1511.0664
    1521.4509                 3056.7199                 3119.2318
    3161.7924                 3614.5141                 3910.7726
Zero-point correction (Hartree): 0.063134

TS.CH3OH+OH.CH2OH+H2O
-------------------------------
E(CCSD(T)/Aug-CC-pVDZ) (Hartree): -191.03690679
E(CCSD/Aug-CC-pVDZ) (Hartree): -191.02050998
     T1 diagnostic:  0.023544
E(MP2/Aug-CC-pVDZ) (Hartree): -190.98071517
E(MP3/Aug-CC-pVDZ) (Hartree): -191.00880732
E(PMP2/Aug-CC-pVDZ) (Hartree): -190.98396957
E(PMP3/Aug-CC-pVDZ) (Hartree): -191.01088144
E(PUHF/Aug-CC-pVDZ) (Hartree): -190.44866616
E(UHF/Aug-CC-pVDZ) (Hartree): -190.44374969
E(CCSD(T)/Aug-CC-pVTZ) (Hartree): -191.20565197
E(CCSD/Aug-CC-pVTZ) (Hartree): -191.18092685
     T1 diagnostic:  0.022051
E(MP2/Aug-CC-pVTZ) (Hartree): -191.14910322
E(MP3/Aug-CC-pVTZ) (Hartree): -191.17265663
E(PMP2/Aug-CC-pVTZ) (Hartree): -191.15257604
E(PMP3/Aug-CC-pVTZ) (Hartree): -191.17482499
E(PUHF/Aug-CC-pVTZ) (Hartree): -190.49695581
E(UHF/Aug-CC-pVTZ) (Hartree): -190.49168506
E(CCSD(T)/Aug-CC-pVQZ) (Hartree): -191.25552981
E(CCSD/Aug-CC-pVQZ) (Hartree): -191.22885767
     T1 diagnostic:  0.021789
E(MP2/Aug-CC-pVQZ) (Hartree): -191.20361394
E(MP3/Aug-CC-pVQZ) (Hartree): -191.22187609
E(PMP2/Aug-CC-pVQZ) (Hartree): -191.20710905
E(PMP3/Aug-CC-pVQZ) (Hartree): -191.22404485
E(PUHF/Aug-CC-pVQZ) (Hartree): -190.50937492
E(UHF/Aug-CC-pVQZ) (Hartree): -190.50407135
E(UM062X/Aug-CC-pVQZ) (Hartree): -191.46043539
Electronic state : 2-A
Cartesian coordinates (Angs):
     C      -0.648965      0.676089      -0.004454
     H      -0.962787      1.249956       0.868940
     O      -1.238637     -0.584747      -0.083491
     H      -0.868492      1.215983      -0.920433
     H       0.493504      0.587300       0.073495
     H      -1.126254     -1.039196       0.753625
     O       1.836377     -0.080561       0.063668
     H       1.575900     -0.748119      -0.590318
Rotational constants (GHz):   26.9959500    5.4928900    4.7961700
Vibrational harmonic frequencies (cm-1):
    i760.7498                   91.5443                  149.1255
     223.1943                  404.1553                  726.7028
    1001.5301                 1078.3864                 1158.3796
    1355.1687                 1404.8678                 1450.1849
    1491.0536                 1760.1556                 3069.6643
    3166.8582                 3781.9194                 3888.8959
Zero-point correction (Hartree): 0.059692

IRC information available
IRCMax information available
E(CCSD(T)/Aug-CC-pVDZ) (Hartree): -191.03668113
E(CCSD/Aug-CC-pVDZ) (Hartree): -191.01977365
     T1 diagnostic:  0.025566
E(MP2/Aug-CC-pVDZ) (Hartree): -190.97969604
```

```
E(MP3/Aug-CC-pVDZ) (Hartree): -191.00705328
E(PMP2/Aug-CC-pVDZ) (Hartree): -190.98366238
E(PMP3/Aug-CC-pVDZ) (Hartree): -191.00955502
E(PUHF/Aug-CC-pVDZ) (Hartree): -190.44519131
E(UHF/Aug-CC-pVDZ) (Hartree): -190.43930455
E(CCSD(T)/Aug-CC-pVQZ) (Hartree): -191.25525482
E(CCSD/Aug-CC-pVQZ) (Hartree): -191.22792783
     T1 diagnostic:  0.023882
E(MP2/Aug-CC-pVQZ) (Hartree): -191.20248982
E(MP3/Aug-CC-pVQZ) (Hartree): -191.21995523
E(PMP2/Aug-CC-pVQZ) (Hartree): -191.20669507
E(PMP3/Aug-CC-pVQZ) (Hartree): -191.22255444
E(PUHF/Aug-CC-pVQZ) (Hartree): -190.50573160
E(UHF/Aug-CC-pVQZ) (Hartree): -190.49947679
E(CCSD(T)/Aug-CC-pVTZ) (Hartree): -191.20535051
E(CCSD/Aug-CC-pVTZ) (Hartree): -191.17999466
     T1 diagnostic:  0.024119
E(MP2/Aug-CC-pVTZ) (Hartree): -191.14797260
E(MP3/Aug-CC-pVTZ) (Hartree): -191.17073752
E(PMP2/Aug-CC-pVTZ) (Hartree): -191.15215430
E(PMP3/Aug-CC-pVTZ) (Hartree): -191.17333528
E(PUHF/Aug-CC-pVTZ) (Hartree): -190.49332545
E(UHF/Aug-CC-pVTZ) (Hartree): -190.48710401
Electronic state : 2-A
Cartesian coordinates (Angs):
     C      -0.643521      0.674339      -0.004799
     H      -0.937038      1.249408       0.874709
     O      -1.241984     -0.577712      -0.083652
     H      -0.851152      1.218255      -0.920942
     H       0.527465      0.555807       0.069479
     H      -1.134023     -1.034256       0.753326
     O       1.826768     -0.082630       0.064053
     H       1.577601     -0.752518      -0.590993
Rotational constants (GHz):   27.2490730    5.5243405    4.8292264

TS.CH3OH+OH.CH2OH+H2O.b
-------------------------------
E(CCSD(T)/Aug-CC-pVDZ) (Hartree): -191.03563250
E(CCSD/Aug-CC-pVDZ) (Hartree): -191.01926707
     T1 diagnostic:  0.023831
E(MP2/Aug-CC-pVDZ) (Hartree): -190.97934715
E(MP3/Aug-CC-pVDZ) (Hartree): -191.00754726
E(PMP2/Aug-CC-pVDZ) (Hartree): -190.98253854
E(PMP3/Aug-CC-pVDZ) (Hartree): -191.00959725
E(PUHF/Aug-CC-pVDZ) (Hartree): -190.44765444
E(UHF/Aug-CC-pVDZ) (Hartree): -190.44284334
E(CCSD(T)/Aug-CC-pVTZ) (Hartree): -191.20429305
E(CCSD/Aug-CC-pVTZ) (Hartree): -191.17961126
     T1 diagnostic:  0.022317
E(MP2/Aug-CC-pVTZ) (Hartree): -191.14766193
E(MP3/Aug-CC-pVTZ) (Hartree): -191.17131880
E(PMP2/Aug-CC-pVTZ) (Hartree): -191.15107086
E(PMP3/Aug-CC-pVTZ) (Hartree): -191.17346215
E(PUHF/Aug-CC-pVTZ) (Hartree): -190.49598333
E(UHF/Aug-CC-pVTZ) (Hartree): -190.49081830
E(CCSD(T)/Aug-CC-pVQZ) (Hartree): -191.25414399
E(CCSD/Aug-CC-pVQZ) (Hartree): -191.22751788
     T1 diagnostic:  0.022061
E(MP2/Aug-CC-pVQZ) (Hartree): -191.20214333
E(MP3/Aug-CC-pVQZ) (Hartree): -191.22050640
E(PMP2/Aug-CC-pVQZ) (Hartree): -191.20557459
E(PMP3/Aug-CC-pVQZ) (Hartree): -191.22264992
E(PUHF/Aug-CC-pVQZ) (Hartree): -190.50841627
```

```
E(UHF/Aug-CC-pVQZ) (Hartree): -190.50321820
E(UM062X/Aug-CC-pVQZ) (Hartree): -191.45910069
Electronic state : 2-A
Cartesian coordinates (Angs):
     C       0.629622      0.656595       0.008737
     H      -0.470824      0.444801      -0.231862
     H       1.000218      1.336005      -0.753678
     H       0.656192      1.127463       0.993345
     O       1.356348     -0.526056      -0.059557
     H       0.982781     -1.160126       0.556348
     O      -1.819132     -0.240785      -0.075075
     H      -2.243832      0.447019       0.460483
Rotational constants (GHz):   28.8162800    5.2052500    4.5898400
Vibrational harmonic frequencies (cm-1):
     i726.1472                57.1726                 113.6145
      220.0909               379.8244                 687.5832
      979.8316              1110.9096                1179.4995
     1314.7005              1395.5790                1432.8677
     1493.4200              1852.5499                3060.3046
     3157.6019              3787.3519                3882.7353
Zero-point correction (Hartree): 0.059473

IRC information available
IRCMax information available
E(CCSD(T)/Aug-CC-pVDZ) (Hartree): -191.03543676
E(CCSD/Aug-CC-pVDZ) (Hartree): -191.01859617
     T1 diagnostic:  0.025706
E(MP2/Aug-CC-pVDZ) (Hartree): -190.97839686
E(MP3/Aug-CC-pVDZ) (Hartree): -191.00593061
E(PMP2/Aug-CC-pVDZ) (Hartree): -190.98222225
E(PMP3/Aug-CC-pVDZ) (Hartree): -191.00836571
E(PUHF/Aug-CC-pVDZ) (Hartree): -190.44443183
E(UHF/Aug-CC-pVDZ) (Hartree): -190.43876210
E(CCSD(T)/Aug-CC-pVQZ) (Hartree): -191.25390416
E(CCSD/Aug-CC-pVQZ) (Hartree): -191.22666942
     T1 diagnostic:  0.024012
E(MP2/Aug-CC-pVQZ) (Hartree): -191.20109667
E(MP3/Aug-CC-pVQZ) (Hartree): -191.21873672
E(PMP2/Aug-CC-pVQZ) (Hartree): -191.20515990
E(PMP3/Aug-CC-pVQZ) (Hartree): -191.22126767
E(PUHF/Aug-CC-pVQZ) (Hartree): -190.50504474
E(UHF/Aug-CC-pVQZ) (Hartree): -190.49900613
E(CCSD(T)/Aug-CC-pVTZ) (Hartree): -191.20402489
E(CCSD/Aug-CC-pVTZ) (Hartree): -191.17875734
     T1 diagnostic:  0.024242
E(MP2/Aug-CC-pVTZ) (Hartree): -191.14660667
E(MP3/Aug-CC-pVTZ) (Hartree): -191.16954828
E(PMP2/Aug-CC-pVTZ) (Hartree): -191.15064652
E(PMP3/Aug-CC-pVTZ) (Hartree): -191.17207813
E(PUHF/Aug-CC-pVTZ) (Hartree): -190.49262468
E(UHF/Aug-CC-pVTZ) (Hartree): -190.48661944
Electronic state : 2-A
Cartesian coordinates (Angs):
     C       0.625042      0.655083       0.008854
     H      -0.502220      0.415617      -0.213849
     H       0.975298      1.334184      -0.763094
     H       0.645759      1.127966       0.992464
     O       1.357280     -0.519861      -0.060668
     H       0.993899     -1.154598       0.561373
     O      -1.809900     -0.242008      -0.075446
     H      -2.242034      0.441283       0.458894
Rotational constants (GHz):   29.0670594    5.2360921    4.6211182
```

```
TS.CH3OH+OH.CH3O+H2O
-------------------------------
E(CCSD(T)/Aug-CC-pVDZ) (Hartree): -191.03211315
E(CCSD/Aug-CC-pVDZ) (Hartree): -191.01400598
     T1 diagnostic:  0.034701
E(MP2/Aug-CC-pVDZ) (Hartree): -190.97367378
E(MP3/Aug-CC-pVDZ) (Hartree): -190.99915664
E(PMP2/Aug-CC-pVDZ) (Hartree): -190.97786609
E(PMP3/Aug-CC-pVDZ) (Hartree): -191.00166923
E(PUHF/Aug-CC-pVDZ) (Hartree): -190.43489454
E(UHF/Aug-CC-pVDZ) (Hartree): -190.42851875
E(CCSD(T)/Aug-CC-pVTZ) (Hartree): -191.20184417
E(CCSD/Aug-CC-pVTZ) (Hartree): -191.17503426
     T1 diagnostic:  0.032928
E(MP2/Aug-CC-pVTZ) (Hartree): -191.14291335
E(MP3/Aug-CC-pVTZ) (Hartree): -191.16377572
E(PMP2/Aug-CC-pVTZ) (Hartree): -191.14729428
E(PMP3/Aug-CC-pVTZ) (Hartree): -191.16636513
E(PUHF/Aug-CC-pVTZ) (Hartree): -190.48371385
E(UHF/Aug-CC-pVTZ) (Hartree): -190.47703717
E(CCSD(T)/Aug-CC-pVQZ) (Hartree): -191.25136376
E(CCSD/Aug-CC-pVQZ) (Hartree): -191.22253676
     T1 diagnostic:  0.032522
E(MP2/Aug-CC-pVQZ) (Hartree): -191.19712582
E(MP3/Aug-CC-pVQZ) (Hartree): -191.21264923
E(PMP2/Aug-CC-pVQZ) (Hartree): -191.20152788
E(PMP3/Aug-CC-pVQZ) (Hartree): -191.21523395
E(PUHF/Aug-CC-pVQZ) (Hartree): -190.49597310
E(UHF/Aug-CC-pVQZ) (Hartree): -190.48926674
E(UM062X/Aug-CC-pVQZ) (Hartree): -191.45815376
Electronic state : 2-A
Cartesian coordinates (Angs):
     C       1.273712      0.382793      -0.020015
     H       1.136011      0.982927      -0.920356
     O       0.403910     -0.718823       0.002903
     H       2.284408     -0.027776      -0.036014
     H       1.158461      1.012782       0.861220
     H      -0.557107     -0.418610       0.341725
     O      -1.623376      0.250957       0.078254
     H      -1.908317     -0.103154      -0.775737
Rotational constants (GHz):   32.6567600    6.4318100    5.6632800
Vibrational harmonic frequencies (cm-1):
    i1311.7676                 125.2912                 185.5549
      225.7753                 409.8703                 785.5099
     1082.5724                1135.2644                1174.2201
     1303.3837                1457.1804                1472.0747
     1512.4416                1696.2149                3042.8788
     3108.5652                3126.1101                3820.1591
Zero-point correction (Hartree): 0.058465

IRC information available
IRCMax information available
E(CCSD(T)/Aug-CC-pVDZ) (Hartree): -191.03183336
E(CCSD/Aug-CC-pVDZ) (Hartree): -191.01339686
     T1 diagnostic:  0.034647
E(MP2/Aug-CC-pVDZ) (Hartree): -190.97334925
E(MP3/Aug-CC-pVDZ) (Hartree): -190.99816720
E(PMP2/Aug-CC-pVDZ) (Hartree): -190.97858191
E(PMP3/Aug-CC-pVDZ) (Hartree): -191.00120067
E(PUHF/Aug-CC-pVDZ) (Hartree): -190.43270968
E(UHF/Aug-CC-pVDZ) (Hartree): -190.42485912
E(CCSD(T)/Aug-CC-pVQZ) (Hartree): -191.25109778
E(CCSD/Aug-CC-pVQZ) (Hartree): -191.22182646
```

```
     T1 diagnostic:  0.032676
E(MP2/Aug-CC-pVQZ) (Hartree): -191.19670111
E(MP3/Aug-CC-pVQZ) (Hartree): -191.21149949
E(PMP2/Aug-CC-pVQZ) (Hartree): -191.20212635
E(PMP3/Aug-CC-pVQZ) (Hartree): -191.21459731
E(PUHF/Aug-CC-pVQZ) (Hartree): -190.49367594
E(UHF/Aug-CC-pVQZ) (Hartree): -190.48553532
E(CCSD(T)/Aug-CC-pVTZ) (Hartree): -191.20160889
E(CCSD/Aug-CC-pVTZ) (Hartree): -191.17437365
     T1 diagnostic:  0.033052
E(MP2/Aug-CC-pVTZ) (Hartree): -191.14253708
E(MP3/Aug-CC-pVTZ) (Hartree): -191.16268719
E(PMP2/Aug-CC-pVTZ) (Hartree): -191.14793964
E(PMP3/Aug-CC-pVTZ) (Hartree): -191.16579006
E(PUHF/Aug-CC-pVTZ) (Hartree): -190.48144373
E(UHF/Aug-CC-pVTZ) (Hartree): -190.47333346
Electronic state : 2-A
Cartesian coordinates (Angs):
     C       1.273864     -0.382078       0.020014
     H       1.137456     -0.979995       0.922016
     O       0.404125      0.718645      -0.004247
     H       2.284370      0.030409       0.035660
     H       1.159118     -1.013164      -0.860423
     H      -0.578921      0.406645      -0.333671
     O      -1.621365     -0.250514      -0.078085
     H      -1.907290      0.103526       0.774988
Rotational constants (GHz):   32.7291721    6.4379865    5.6695878
```